J. Astron. Space Sci. 18(3), 191–208 (2001)

# TERRESTRIAL IMPACT CRATERING CHRONOLOGY: A PRELIMINARY ANALYSIS

**Hong-Kyu Moon[1†], Byung-Hee Min, André B. Fletcher, Bong-Gyu Kim Wonyong Han, Moo-Young Chun, Young-Beom Jeon, Woo-Baik Lee**

Korea Astronomy Observatory, Yusong, Taejon 305-348, Korea

email : fullmoon@kao.re.kr, bhmin@kao.re.kr, abfletch@kao.re.kr

*(Received November 15, 2001; Accepted November 30, 2001)*

## ABSTRACT

We have recently compiled a database of the properties of 192 impact craters, which supercedes previous compilations. Using our database, the impact structures found in North America, Europe and Australia have been examined; these cratonic areas have been relatively stable for considerably long geological periods, and thus have been best preserved. It is confirmed that there is a close correlation between the geological epoch boundaries, the epochs of mass extinctions, and the "timing" of impacts. In addition, the terrestrial cumulative flux of objects >20km is found to be $1.77\times10^{-15}$km$^{-2}$yr$^{-1}$, over the last 120 Myr, which is much smaller than the published values in McEwen et al. (1997) and Shoemaker (1998) ($5.6\pm2.8\times10^{-15}$km$^{-2}$yr$^{-1}$). For terrestrial impact structures with D>50 km, the apparent cumulative flux over the last 2450 Myr is ~50 times smaller than the corresponding value for the Moon. If we assume that the Earth and the Moon suffered the same level of bombardment over this time, this would mean that the actual flux of impacting bodies, capable of making craters with D>50 km, was ~ 50 times larger than the apparent flux estimated from the currently known terrestrial records.

*Keywords*: terrestrial impact craters, geological epochs, erosion, global mass extinction

## 1. INTRODUCTION

Our Earth is subject to violent planetary processes, such as the impacts of comets and asteroids. Compared to the Moon, planet Earth has been bombarded more heavily over the course of its geological history, due to its stronger gravity. However, much of the terrestrial impact record has been modified, or even erased, by active geological processes: Earth's crater record is totally different from that of the Moon, which has been supersaturated with impacts. The explosive nature of a collision, in the context of Solar System evolution, comes from the very high velocity with which an interplanetary object may hit a planet. The velocity of an Earth-impacting projectile can range from 11.2 km s$^{-1}$ (Earth's escape velocity) to 72 km s$^{-1}$ (Earth's orbital velocity plus the escape velocity of an object 1 A.U. distant from the Sun). Since the kinetic energy liberated by an impact is proportional to the square of the projectile's velocity, the destructive power of, say, a 10 km-sized minor planet is enough to cause mass extinction of terrestrial life, on a global scale.

†corresponding author

The population of terrestrial impactors forms a quasi-power-law size distribution, extending from diameters of a few meters to larger than 10 km. Numerous impacts have occurred over the Earth's lifetime (i.e. the last ~4.6 Gyr or so). From the recorded properties of the impact craters formed by such events, one can estimate the apparent frequency and time distribution of impacts, and infer the characteristics of interplanetary projectiles, as well as their physical consequences for our Earth, on a global scale over geological time.

Terrestrial erosion processes, combined with plate tectonic activity, have helped reveal some of the impact craters' subsurface structures, which include highly shocked and shock-melted materials which had previously been hidden beneath the Earth's crust (Schnetzler & Honey 1998). Though there is an abundance of ground-based data available from the major impact sites, little attention has been given, until recently, to the application of remote sensing techniques to this research field. This is in sharp contrast to the considerable achievements made by the digital image mapping of the terrestrial planets. However, it should be noted that, in recent years, some 3 to 5 new impact craters are detected every year during routine observations by orbiting satellites and space shuttles.

Because impact projectiles strike the Earth in essentially random fashion, the resulting impact sites would be expected to be uniformly distributed over the Earth's surface. However, the currently recorded ground distribution of craters is far from random, with major concentrations occurring in North America, Europe, Australia and Russia. By contrast, there are cratonic areas in other parts of the world, where relatively few impact sites have so far been found, e.g. Africa and South America. This is because we have far less information on the impact structures in these particular cratons, mainly due to serious difficulties in our physical access to the "missing craters". For example, in Africa, possible impact structures detected by orbiting vehicles have not yet been explored on the ground. Craters in remote areas, such as desert regions and tropical jungles, will continue to remain effectively inaccessible to ground-based investigations. Furthermore, ongoing wars, restrictive policies imposed by governments or private mining companies, funding shortages, and the lack of usable infrastructure, are all common problems which block the investigation of possible impact craters in "difficult" regions, such as Africa (Master & Reimold 2001).

## 2. THE DATA

To date, some 250 terrestrial impact structures have been cataloged by individuals and a few research groups. In this preliminary study, we compiled up-to-date listings (e.g. from Grieve 1991, Hodge 1994, Fortes 2000, and Moilanen 2001) of the properties of 245 impact craters; from these data, we selected 192 impact structures with "well-constrained" properties (namely, their diameters and ages). We classified the remaining 53 structures as "probable" or "possible" impact craters, based on the uncertainties in their recorded properties. The data compiled in our crater listing has never before been assembled into a single body of information: our database thus supercedes previous compilations (i.e. Grieve 1991, Hodge 1994, Fortes 2000, and Moilanen 2001), and it reflects recent additions and corrections to the previously available data. The impact craters in our database have ages ranging from 0–2500 Myr, and diameters from $D<1$ km to $D>300$ km. The purpose of this preliminary study is to establish a starting point for the understanding of terrestrial impact cratering processes, via systematic analyses of the available ground-based data. In interpreting the terrestrial impact cratering record, it is important to note that it suffers from multiple, serious biases, many of which do not occur in the lunar record.

All entries in our database have diameters $D>5$ m. For multiple-impact craters found in the same craterfield, we listed only the largest such structure, even if the multiple-impact group had been formed from the same initial projectile. For example, Sikhote Alin (Krinov 1971) has as

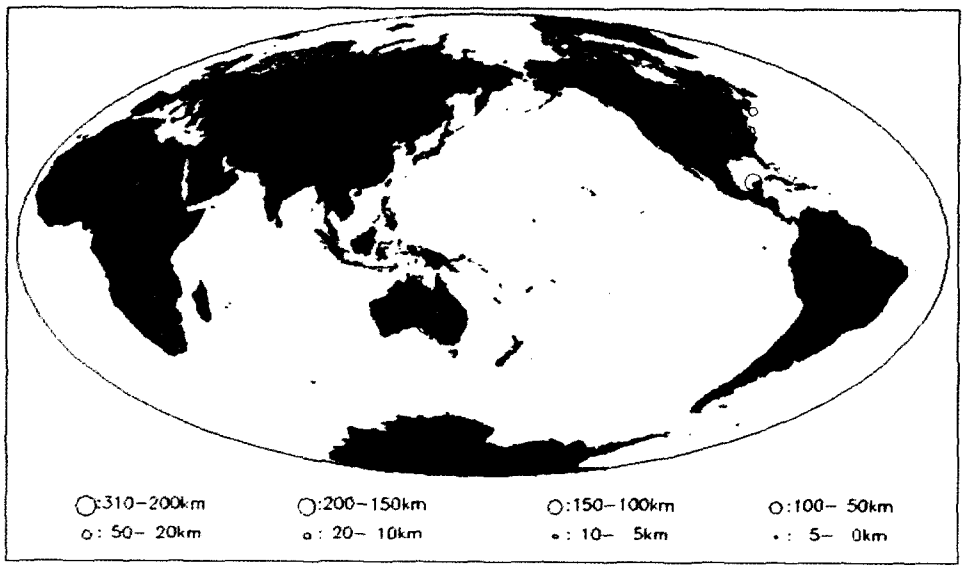


Figure 1. Locations and diameters of known terrestrial impact craters (2001).

many as 120 craters (or pits), of which 36 have diameters D>5 m. Also, we listed multiple-impact craters with D>1 km as an individual impact structure (e.g. the Reis-Steinheim pair in Germany; the Clearwater East-Clearwater West pair in Canada; and the Kara-Ust Karat pair in Russia).

For diameters D<20 km, most of the impact structures fall below the basic power-law distribution, with increasing statistical incompleteness towards smaller sizes: smaller events are more frequent than medium-sized events, which, in turn, are much more frequent than large impacts capable of producing craters with, say, D>100 km. It seems that the impact crater "preservation probability" increases with size: smaller structures are much more easily erased than larger ones (Montanari et al. 1998). The size-frequency distribution of the currently known terrestrial craters suggests that the apparently low cratering frequency for the smaller craters would not be dramatically increased, even with much improved statistics. Nevertheless, it is the larger impacts which count for much more in the study of impact cratering history, and of the possible cause-and-effect relationships between impacts and massive ecological crises. Hence, giant impacts often leave a global signature in the geological record, and have world-wide climatic, biological, and ecological effects. A detailed analysis of impact crater properties, such as their location, age, and size, is required to estimate the actual flux of impacting bodies, as a function of time. As a first step, the apparent flux may be estimated from our database. Then, the various biases in the terrestrial record need to be estimated, before they can be corrected for in the final calculation of the actual terrestrial impact flux (which, in general, will be a function of at least 2 parameters: time, and projectile size). At the same time, we plan to actively maintain and update our database, so as to keep track of the growing body of information accumulated from the terrestrial cratering record.

Fig. 1 is an Aitoff projection plot showing the locations and diameters of currently known (i.e. as of 2001) terrestrial impact craters. The crater diameter is indicated by the plotting symbol size,

according to the legend at the bottom. The red circles are the older data from Grieve (1991); newer data are plotted using yellow circles. With the addition of these data, our up-to-date compilation has statistics which are a significant improvement over previous listings. From Fig. 1, we see that the majority of impact craters are located in North America, Europe, and Australia. These regions are known to be geologically stable cratons, and they have been better mapped than other areas, because more active and efficient search programs have been underway there, since 1980's.

## 3. THE CRATERING RECORD AND ITS UNCERTAINTIES

The primary source of uncertainty in the impact structure database is the statistical incompleteness of the cratering record. Though visible impact craters are specifically a surface phenomenon, buried structures account for about 20% of the currently known terrestrial record: initially, most of them were detected as gravitational anomalies, and were later drilled to confirm their impact origin (Grieve 1991). The Earth's surface is dynamic on geological timescales: hence, terrestrial craters have complex post-impact histories involving erosion, sedimentation, vegetation, plate tectonic and, probably, volcanic activities. These are the major reasons why the terrestrial impact record has strong, multiple biases which make clear, direct interpretations difficult.

For our analysis, we decided to include impact structures found in North America, Europe and Australia, as they have been stable against erosional processes for considerably long geological periods, and they are areas in which active search programs have been underway, for some time now. Since our data has been collected from various, heterogeneous sources, several different methods had been employed to measure the diameters: some impact craters could be measured from rim to rim, while others could only be measured using the gravitational anomalies resulting from the impact. In most cases, original rim diameters were reconstructed; only a small fraction of craters, with minimal information, have considerable uncertainties in their individual estimates (Grieve 1991). This leads to large error margins in the crater size, since the different individual estimates may yield significantly discrepant results. For example, early estimates of the Chicxulub crater, based upon gravity anomalies and aeromagnetic data, indicated a 180-200 km diameter structure (Hildebrand et al. 1991), while further processing of the same data led to a proposed estimate of ~300 km (Sharpton et al. 1993). In this study, we adopt conservative values for each crater (for Chixculub, we chose the smaller diameter, i.e. 180 km), following the tradition adopted by previous researchers.

Age bias is also significant, because each impact crater datum is associated with a particular geological epoch. An impact age may be determined by a variety of methods; however, precise ages are known for only about one third of the currently known sample. Precise timing involves radiometric dating of the impact melt rocks or glasses, or a biostratigraphic method applied to impact ejecta placed within a well-defined stratigraphic sequence. Ejecta, which are found in a sedimentary layer with the biological signatures of an impact, may be dated (in units of Myr); this allows the "timing" of the impact relative to the nearest geological epoch boundary to be determined. In general, the most reliable dating is given by a radioisotopic analysis of the crater's melt rock (Montanari et al. 1998). Most craters are found on land, yet they are liable to be buried or filled by irregular sequences of sediments, which makes direct stratigraphic comparison with marine fossil records very difficult. On the other hand, sequences of marine sediments are dated by interpolating a few radioisotopic ages determined from collections of interbedded volcanic ashes found in various, distantly separated, parts of the world. After that, the marine records may be compared with paleontological, geochemical and geophysical signatures, which are presumed to have occurred at the same time. According to Montanari et al. (1998), the link between an impact and an apparently contemporaneous impact signature found in the sedimentary record depends on the precision of the

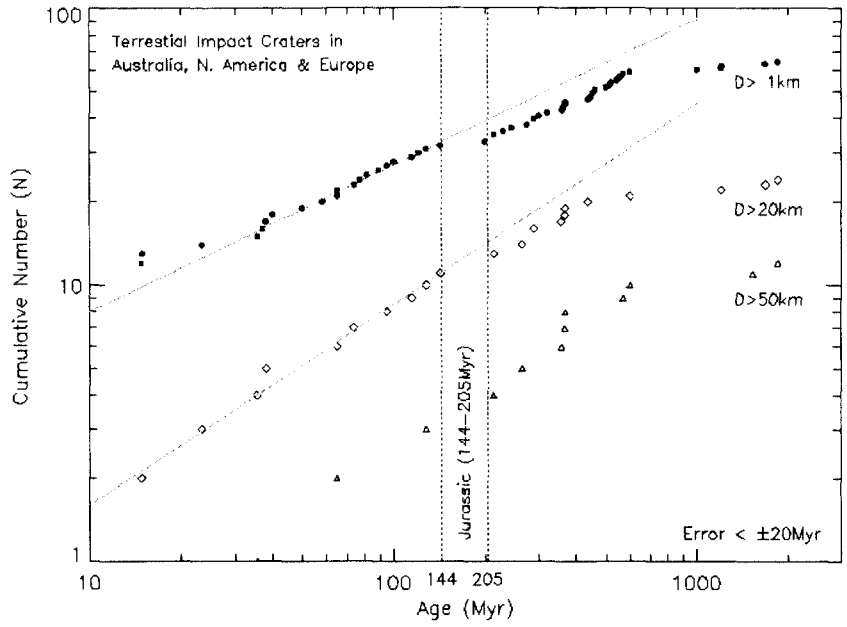


Figure 2. Cumulative number vs. age for terrestrial impact craters in N. America, Europe and Australia (2001).

geochronologic timescale calibration, as well as on the accuracy of the impact crater dating.

Fig. 2 shows a plot of the cumulative number vs. age for terrestrial impact craters found in North America, Europe and Australia, restricted to those which have well-defined ages (i.e. with uncertainties <20 Myr). In this log-log plot, the cumulative number is counted back to the start of the Precambrian era (~2.4 Gyr ago), and the cumulative number increases roughly as a power law with age, up to t~144 Myr. Among these three cratonic areas, Australia is very important, as it is one of the most geologically stable continents: it has an impact record going back into the Precambrian era, which spans more than 10% of Earth's history (Shoemaker 1998). The crater records become much more poorly sampled beyond an age of t~600 Myr (i.e. in the Precambrian era). In this plot, the black circles represent the cumulative counts for craters with D>1 km, while the diamonds are for D>20 km. We fit two straight lines (i.e. power laws) to the D>1 km and D>20 km data, restricting the fits to ages t<144 Myr. There is a definite break at t~144 Myr, for all diameter cutoffs, when the apparent cratering rate suddenly increased. This break occurs sometime in the Jurassic era (144-205 Myr), during which an apparent deficit in the terrestrial impact cratering rate seems to have occurred: there are remarkably few new craters formed in this period (see Fig. 4). Thus, we may assume that we have an incomplete crater sample over at least part of the Jurassic era. Pre-Jurassic craters may have suffered significantly more from the accumulated effects of eroding processes, which would make them much harder to find: this may explain the apparent decrease in the impact cratering rate. Within our new dataset, the "well-preserved" craters are found with ages up to at least t~144 Myr, which is beyond the previously estimated transition point (i.e. t~120 Myr) discovered by Grieve & Shoemaker (1994). This plots shows the raw data, as of 2001; no corrections for observational biases have been made in this preliminary study. In fact, the recent crater "preservation period" may

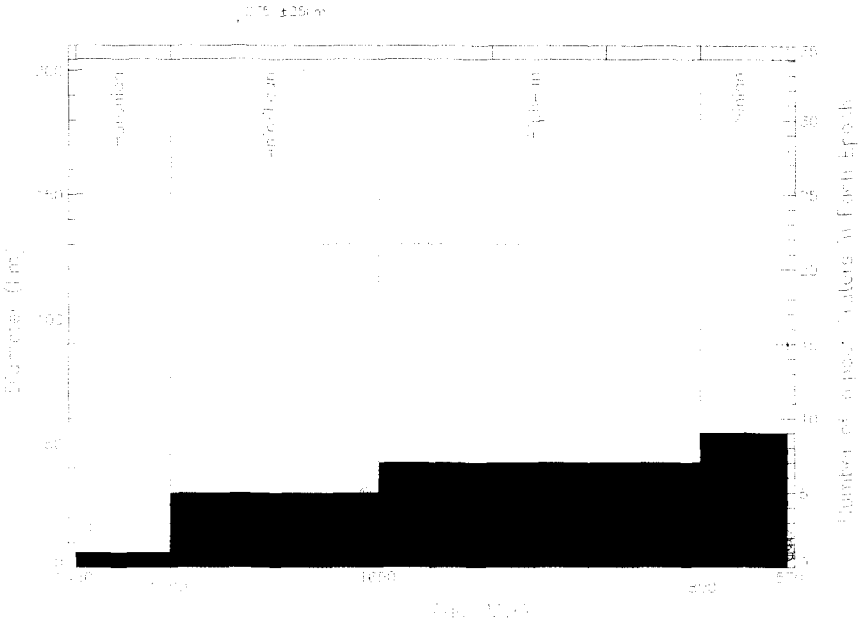

Figure 3. Number and diameter vs. age: terrestrial impact craters in the Precambrian era (2450-570 Myr).

continue back to as far as t~205 Myr, but this cannot be accurately determined from our current database, as there are relatively poor crater statistics for the intervening Jurassic period.

## 4. THE IMPACT CRATERING CHRONOLOGY

Major impacts, capable of forming craters as large as the Chicxulub structure (D>100km), have occurred many times over Earth's history. These enormously energetic events have been found to have strongly affected the evolution of the biosphere, on both local and global scales. In this section, we briefly review the Earth's impact record, and the biological effects of the impacts, with emphasis on the ecological catastrophes. With our newly compiled database in hand, we examined the number and diameter distributions of the craters, as a function of geological epoch. Figs. 3, 4 & 5 show the age distribution of the crater impacts in the database, plotted as a function of time (i.e. the geologically determined age; see Herland et al. 1990, Gradstein et al. 1995). These plots display the diameter (left vertical scale) vs. age for currently known terrestrial impact craters with ages between 570 and 2450 Myr (Precambrian epochs) (Fig. 3); 248 to 570 Myr (Cambrian to Permian epochs) (Fig. 4); and 0 to 248 Myr (Triassic to Quaternary epochs) (Fig. 5). The relative durations of the 3 periods covered in these figures are: 100:17:13, respectively (for clarity of presentation, different nonlinear time scales had to be chosen for each of these 3 figures). Superimposed on the age distribution is the histogram of the total number of craters (right vertical scale) with ages within the indicated major geological epochs. For comparison, a histogram, in dashed lines, is also drawn, corresponding to the older data listing compiled by Grieve (1991). The uncertainty (or limit) for each crater's age is plotted; since accurate impact timing is not generally possible for the older features,

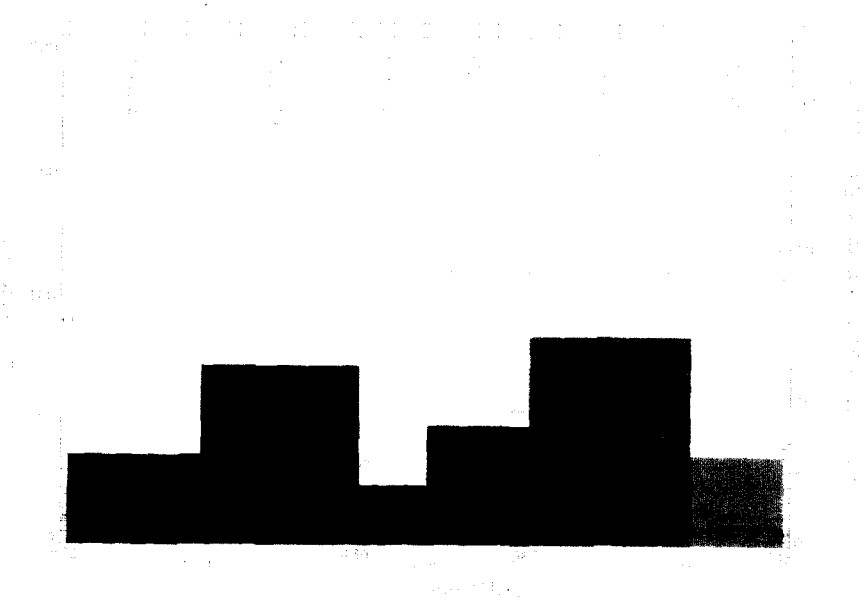

Figure 4. Number and diameter vs. age: terrestrial impact craters in the Cambrian to Permian epochs (570-248 Myr).

the age uncertainties can sometimes be relatively very large.

The top bar indicates both the major and minor (fine-scale) divisions of geological time. The vertical dashed lines delineate the major geological epoch boundaries. We define the "Doomsday Craters" to be those with D>50 km; these are indicated by the red symbols (see the Appendix for our newly compiled list of 192 craters; 20 of these are "Doomsday Craters"). It has been more than a decade since Jansa et al. (1990) proposed the minimum projectile size which could produce a global mass extinction; they deduced a zero extinction threshold (diameter) for the impact projectile to be 3 km (this would produce a crater diameter of ~45 km); we adopted D=50 km as the zero extinction threshold diameter for the "Doomsday Craters". It is widely accepted that about 50% of marine extinction could occur as a result of an impact of a 10 km-sized object, the size of which would be comparable to the comet or asteroid that caused the Chicxulub crater, some 65 Myr ago (Montanari et al. 1998, and references therein). The most important aspect of Figs. 3, 4 & 5 is the tight correlation between stratigraphic and paleontological records in the geochronologic timeframe where the impact crater record is based (see, e.g., Hildebrand 1993, Montanari et al. 1998, Dypvik & Attrep, Jr. 1999). In this preliminary study, we confirmed 20 "Doomsday Craters" (see Figs 3 – 5, and also the Appendix). We also found that 45% of them (i.e. 9 craters) were formed at geological epoch boundaries, in the last 144 Myr (i.e. from the J/K boundary to the Quaternary era).

There is large quantity and variety of concordant evidence for the coincidences of impact times with known geological and ecological signatures of mass extinction. We provide some examples here: the Acraman structure, with an age >570 Myr, was found to have a high iridium anomaly (Gostin et al. 1989), and we conjecture that this crater's age coincides with the Sinian-Cambrian epoch boundary. On the other hand, Joachimski & Buggisch (2001) claimed that there is no clear evidence for an impact in the late Devonian mass extinction (~ 363 Myr); however, Claeys et al.

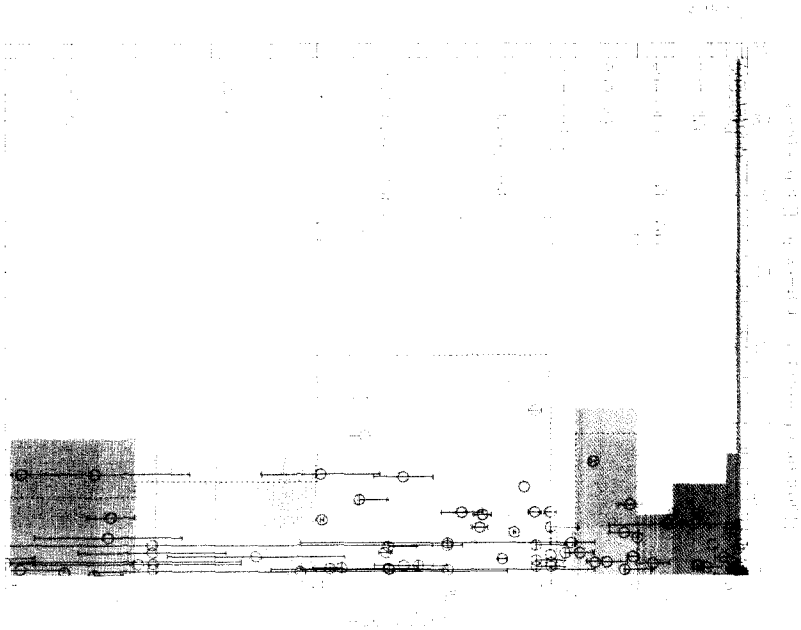

Figure 5. Number and diameter vs. age: terrestrial impact craters in the Triassic to Quaternary epochs (248-0 Myr).

(1992) proposed that the Siljan Ring (368 Myr) and Charlevoix (357 Myr) structures have the characteristics of an impact origin. Also, for the Alamo crater (367 Myr), Morrow & Sandberg (2001) concluded that an extraterrestrial body struck relatively deep water in the early part of the Late Devonian period. Glikson et al. (2001) identified the Woodleigh crater as resulting from a possible impact at the Permian-Triassic boundary, which then caused a global mass extinction. Further, McDonald et al. (2000) found evidence for an L-Chondrite impact projectile in the Morokweng crater, and they concluded that a giant impactor hit the Earth at the J/K epoch boundary. The timing of the impacts of the Duolon (129 Myr) and Tookoonooka (128 Myr) structures corresponds to the EA epoch boundary. Likewise, the Popigai (35.7 Myr) and Chesapeake Bay (35.5 Myr) craters are thought to be the main cause of the LE epoch boundary.

Since precise impact timing is not always possible, especially for structures older than $\sim$144 Myr, it is difficult to correlate geological epoch boundaries with the impact "dates" for the much older craters. It is interesting to note that there are remarkably few Jurassic craters. Also, in the last $\sim$ 5 Myr, there has been a marked increase in the apparent cratering flux. This is almost certainly due to the minimal amount of erosion incurred by these relatively young impact sites. From Figs. 3, 4 & 5, we find that the terrestrial cratering record has been far from "steady" over the last 2450 Myr; it shows 4-5 apparent peaks (i.e. in the Ordovician, Carboniferous, Cretaceous, Eocene, and Quatenary eras) of higher cratering intensity.

Fig. 6 is an Aitoff projection plot showing the locations and ages of the currently known impact structures in our database. The crater age is indicated by the plotting symbol shape, according to the legend at the bottom. In particular, the crater impacts at the J/K and K/T geological time boundaries

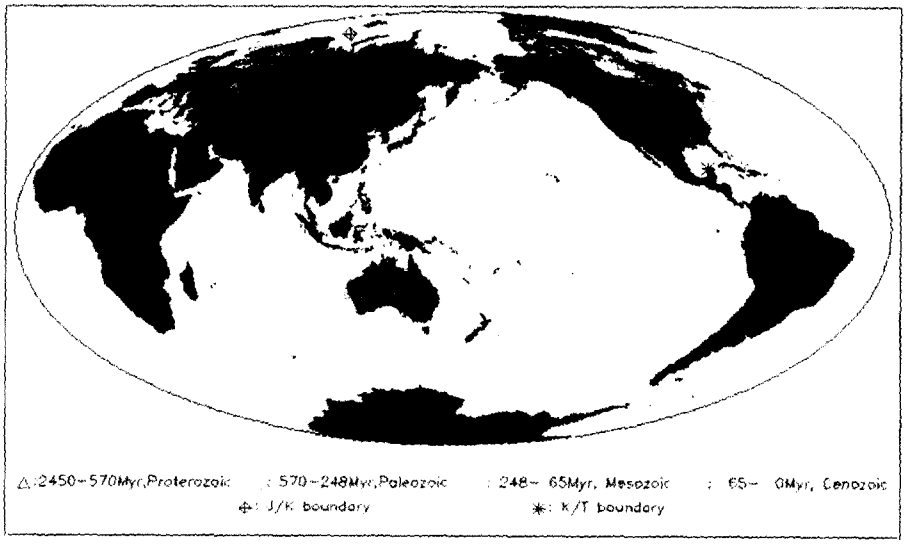


Figure 6. Locations and ages of currently known terrestrial impact craters.

are assigned their own symbols. Note that North America, Europe and Australia have relatively abundant impact structures, as they are well-surveyed, as well as geologically stable, cratons.

## 5. THE CUMULATIVE FLUX IN 3 WELL-SURVEYED CRATONIC AREAS

In Fig. 7, we plot the cumulative flux vs. size (i.e. diameter) distribution (FSD) of those terrestrial impact craters found in the 3 well-surveyed cratons (North America, Europe and Australia), with age uncertainties <20 Myr. We divided these data into 2 groups, according to age: recently created impact craters (age $t<144$ Myr), and all the older ones (age $144<t<2450$ Myr). The top right inset table shows the symbols used for each age-location pair. The 144 Myr age cutoff, which is near the J/K boundary, is 24 Myr earlier than the 120 Myr value previously used by McEwen et al. (1997) and Shoemaker (1998). This plot shows that the terrestrial impact cratering rate has apparently increased by about an order of magnitude within the last 144 Myr, as compared with the overall rate for previous epochs. With these more abundant data for the recent geological epochs, it is clear that, while both North America and Europe are very similar in their detailed FSDs, the Australian FSD is qualitatively very different. We note that there is about double the apparent cratering rate for the small craters, and a relatively lower apparent rate for the large craters in this cratonic region (there is a sudden drop in the cratering flux at D~1 km, and there are no known craters larger than D~70 km). On the other hand, the apparent cratering fluxes in both North America and Europe are also similar to the cumulative flux summed over all 3 cratonic areas. From Fig. 7, we see that both the North American and European FSDs have a gently sloping flux "plateau" below about D~3 km.

In Fig. 8, we plot the FSDs for terrestrial impact craters with various age (120, 144, 2450 Myr) and size (1, 20, 50 km) cutoffs. The age uncertainty of these data is <20 Myr. These FSDs clearly show that, in recent geological history ($t<144$ Myr), the apparent cumulative flux has increased by almost an order of magnitude, as compared to the corresponding (apparent) flux estimated using the

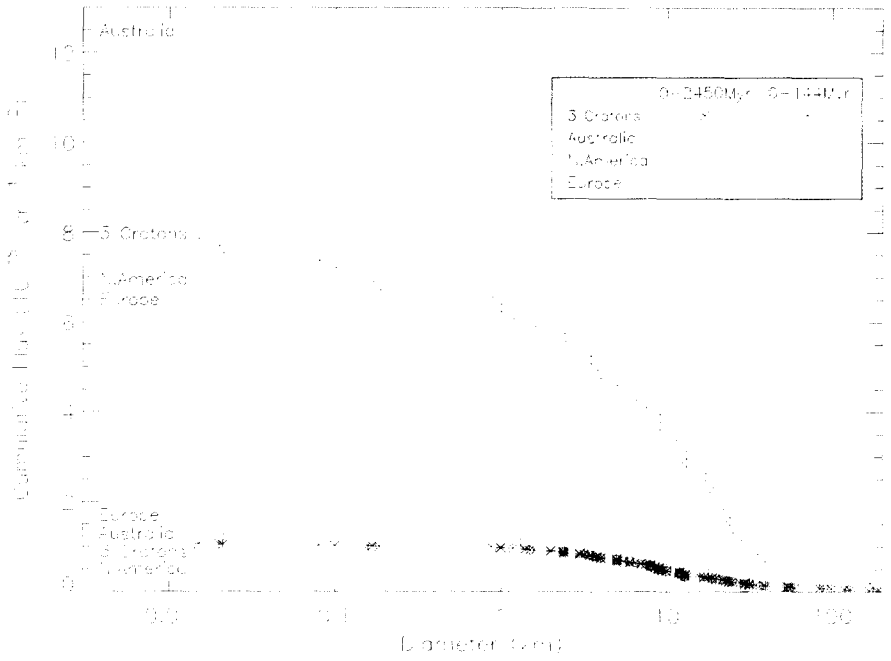

Figure 7. Cumulative flux vs. diameter for terrestrial impact craters in North America, Europe and Australia.

entire geological record (t<2450 Myr). This age bias is probably due to known active geological processes native to the Earth, especially those in the pre-Cretaceous period. The previous result of McEwen et al. (1997) ($5.6\pm2.8^{-15}$yr$^{-1}$km$^{-2}$) has a large uncertainty, and so is not inconsistent with our best current estimate of the cumulative flux for D>20 km craters ($1.77\times10^{-15}$yr$^{-1}$km$^{-2}$). However, the discrepancy between our cumulative flux and that of McEwen et al. (1997) arises from the significant growth in the available data on impact craters, in recent years. The apparent break in the FSDs, at a crater diameter of D~1 km (we note from Fig. 7 that the actual break is at D~7 km), implies that the smaller craters must have been more efficiently "erased" from the record. The fact that there is a clear break for both young and old craters means that the more efficient "vanishing" of the smaller craters holds irrespective of crater age.

## 6. THE CUMULATIVE FLUX VS. DIAMETER DISTRIBUTION IN THE EARTH-MOON SYSTEM

Planetary impact cratering records can provide an overall picture of bombardment, integrated over the lifetime of the impact surfaces studied. With the advent of space science missions, a direct comparison of the terrestrial and lunar impact crater records became possible. Further, it should be noted that the FSD of lunar craters may be used as a "control" sample for terrestrial impact studies, since the lunar surface has been unaffected by erosion, deposition, and tectonic drift (Strom 1998), nor by volcanic activity. Because the process of crater formation appears to be time-dependent, we may attempt to infer the population and evolution of the Solar System's minor planets (Neukum et

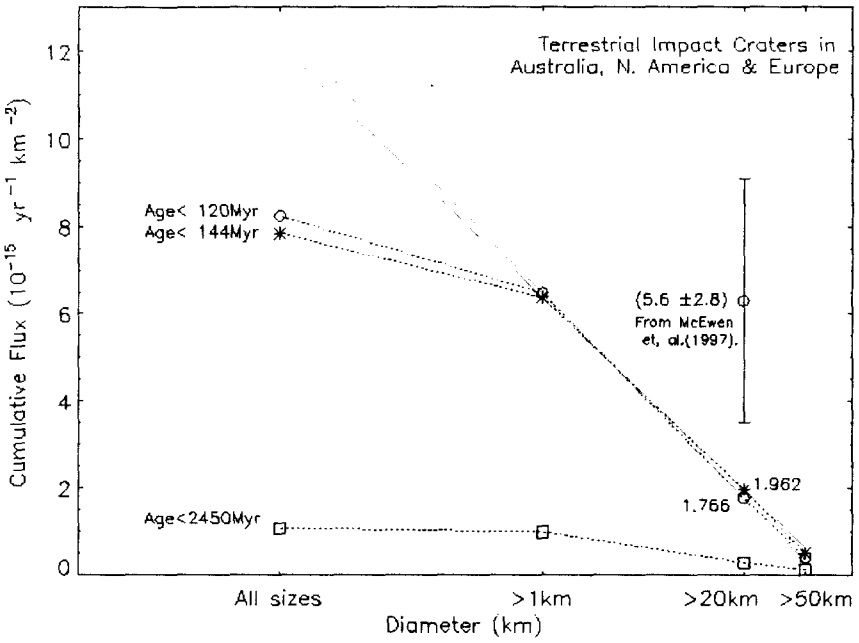


Figure 8. Cumulative flux vs. diameter for terrestrial impact craters, with various age and diameter cutoffs.

al. 2001) from the lunar records. In Fig. 9, we plot the FSD for both lunar and terrestrial impact structures with D>50 km. The terrestrial diameter FSD is plotted using 3 different cutoff ages (120, 144 & 2450 Myr). Likewise, the FSD for 753 lunar impact structures with D>50 km (the "Principal Lunar Craters"; U.S. Geological Survey 2001) are also plotted. For airless planets, a surface age of 3.9 to 4.0 Gyr is widely accepted (Hartmann et al. 2001), so we adopt an age of 3.95 Gyr for the Moon. However, the lunar surface age varies from region to region: the oldest areas are probably ~4.6 Gyr old. Thus, the current estimates of the lunar cumulative impact flux should be taken as upper limits.

From Fig. 9, it is evident that the cumulative impact flux on the lunar surface is much larger than the corresponding flux on the Earth. For craters with D>50 km, the apparent cumulative lunar flux (over the past ~3950 Myr) is at least ~50 times larger than the apparent cumulative flux on the terrestrial surface (over the past ~2450 Myr). This is probably due to the long-term absence of active geological processes (e.g. erosion, sedimentation, vegetation, plate tectonic dynamics and volcanic activity) on the Moon. The FSD steepens greatly for mid-sized lunar craters with D<100 km; if the trend for these craters is extrapolated to larger diameters, there is clearly a significant excess of large lunar craters (a similar excess appears in the Earth's crater record: see Fig. 7). Thus, the formation rate of large impact craters is relatively high compared with that for smaller craters, for both the Earth and Moon. This may imply that there was a large population of giant impactors in the history of the inner Solar System.

The land surface area of the Earth is ~13 times that of the Moon. Also, the total area of the Earth's ocean floor is >4 times that of the Moon, although ocean floor impact structures are currently almost completely undiscovered. If a new method is developed for the detection of impact signatures

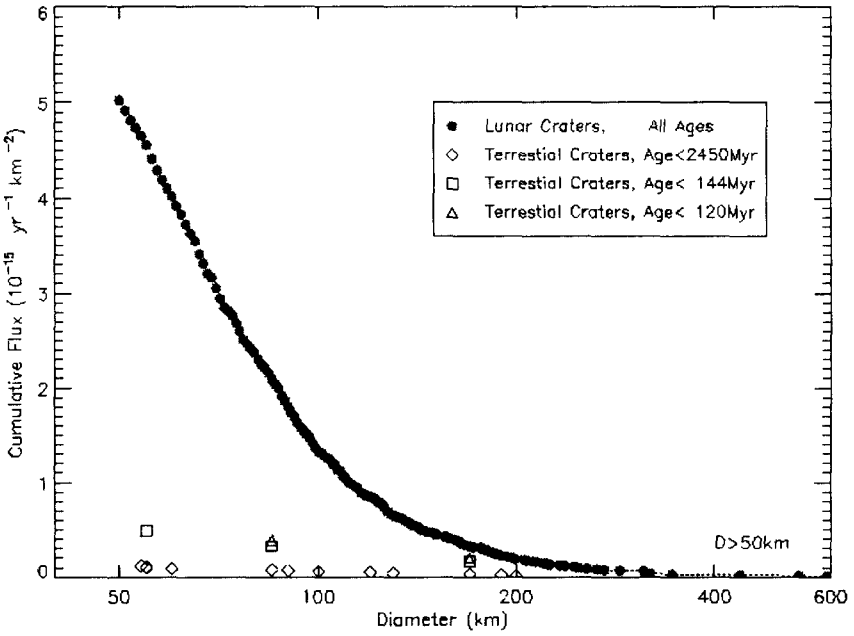


Figure 9. Cumulative flux vs. diameter distribution for lunar and terrestrial impact craters.

on deep ocean beds, a more accurate FSD could be obtained for the terrestrial surface record.

## 7. CONCLUSIONS

In this preliminary study, we compiled a catalog of terrestrial impact craters, from which we selected 192 "well-defined" impact features whose diameters and ages are relatively well-constrained. Our new database supercedes previous listings (i.e. Grieve 1991, Hodge 1994, Fortes 2000, Moilanen 2001), and the resulting statistics have significantly improved with the recent additions and corrections to the previous datasets. Due to active geological processes, such as erosion, sedimentation, vegetation, and the destructive effects of plate tectonic and volcanic activity, terrestrial impact records have been modified, or even erased, over the course of Earth's geological history. The inherent uncertainty and paucity of age data reflects both the lack of detailed studies, as well as of datable material, particularly for deeply eroded or subsurface structures. Furthermore, about 2/3 of the Earth's crust is covered by water, so there is a 2:1 chance that an Earth-impacting asteroid or comet would land in an ocean. Almost nothing is currently known about craters on ocean basins, so we are left with statistics for only those on the Earth's land crust (Shoemaker 1998). Thus, in future, systematic efforts to search for impact structures on ocean beds, as well as on relatively less well-surveyed land areas, are needed.

In general, an impact structure is identified not only by its morphology, but also by its geological, chemical and geophysical properties. We examined the properties of impact craters found in North America, Europe and Australia. These cratonic regions have been relatively stable, with low rates of active geologic processes, and they are also areas in which active search programs have been

underway for some time. With our newly compiled database, we examined the number and diameter distributions of terrestrial craters, as a function of geological epoch.

In our preliminary analysis, we find close correlations between the geological epoch boundaries, the epochs of mass extinctions, and the "timing" of crater impacts. Terrestrial impacts are responsible for the mass extinction event ~65 Myr ago, which saw the final demise of the dinosaurs. Such a catastrophe can strongly affect the ecological system (i.e. the biosphere and the environment) on both local and global scales. The majority of "Doomsday" impacts occur at geological epoch boundaries, while those in the intervening periods are usually in the small and medium size ranges. We confirm 20 "Doomsday Craters" (which we define to have D>50 km) in our study, and we find that ~45% of them were formed at or near geological epoch boundaries. Since precise impact timing is not always available for the relatively old structures, it would be impossible to perform a useful correlation with the known geological time boundaries for these much older craters. At the very least, it is clear that the terrestrial impact cratering flux has been far from steady over the last ~2450 Myr, as it has peaked at least 4-5 times.

The cumulative flux-size (FSD) distribution shows that, in recent geological history, the apparent cumulative terrestrial flux has increased by almost an order of magnitude relative to the corresponding flux for the entire geological record (age <2450 Myr). With the more abundant data for recent epochs, it is clear that, while both North America and Europe are very similar in their detailed distribution of impact fluxes as a function of crater diameter, the Australian FSD is qualitatively very different. Thus, it is evident that impact structures found in different locations in the world have had different erosion rates, which leads to each craton having a different impact cratering record, as observed at the current time. In addition, there is a marked increase in the apparent cratering flux within the last ~5 Myr. This is almost certainly due to the minimal amount of erosion incurred by these "fresh" impact sites.

We find that the cumulative flux of objects with D>20km, to be $1.77\times10^{-15}$km$^{-2}$yr$^{-1}$, over the last 144 Myr, which is much smaller than the published values in McEwen et al. (1997) and Shoemaker (1998) ($5.6\pm2.8\times10^{-15}$km$^{-2}$yr$^{-1}$). For terrestrial impact structures with D>50 km, the apparent cumulative flux, over the past ~2450 Myr, is ~50 times smaller than the corresponding value for the Moon. If we assume that the Earth and Moon have suffered the same level of bombardment, i.e. identical actual impact cratering fluxes, this preliminary result implies that the actual flux of impactors, capable of making craters with D>50 km, was about ~50 times larger than the apparent flux estimated from the currently known terrestrial records. The shape of the lunar crater FSD becomes much steeper below D<100 km, and there is a clear excess of larger craters (D>100 km) relative to the smaller ones. This is also observed for the terrestrial craters. Thus, there may have been a large population of giant impacting bodies in the history of the inner Solar System.

We will maintain an active database of impact structures, to keep track of the growing terrestrial record. This program will, in future, improve the statistics of the terrestrial impact record, and thus deepen our knowledge of planet Earth's geological history.

**ACKNOWLEDGEMENTS:** This paper is supported by the National Research Lab (NRL) of the Korean Ministry of Science and Technology (MOST). We acknowledge J.-M. Kyeong, who helped with the preparation of the final LaTeX document.

## REFERENCES

Claeys, P., Casier, J.-G., & Margolis, S. V. 1992, Nature, 257, 1102
Dypvik, H., & Attrep, M., Jr. 1999, M&PS, 34, 393

Fortes, A. D. 2000, Terrestrial Impact Structures, http://planetaryweb.ucl.ac.uk/crater.htm
Glikson, A. Y., Mernagh, T. P., Mory, A. J., Iasky, R. P., & Pirajno, F. 2001, Ceme. Conf., 3044
Gostin, V. A., Keays, R. R., & Wallace, M. W. 1989, Nature, 340, 17
Gradstein, F. M., Agterberg, F. P., Ogg, J. G., Hardenbol, J., van Veen, P., Thierry, J., & Huang, Z. 1995, in Geochronology, Time Scales, and Global Stratigraphic Correlation, eds. Bergren, W. A., Kent, D. V., Aubry, M.-P., & Hardenbol, J. (Boulder: Society for Sedimentary Geology), 95
Grieve, R. A. F. 1991, Meteoritics, 26, 175
Grieve, R. A. F., & Shoemaker, E. M. 1994, in Hazards due to Comets and Asteroids (AZ: University of Arizona Press), 417
Hartmann, W. K., Anguita, J., de la Casa, M. A., Berman, D. C., & Ryan, E. V. 2001, Icarus, 149, 37
Herland, W. B., Armstrong, R., Cox, A., Lorraine, C., Smith, A., & Smith, D. 1990, A Geologic Time Scale (New York: Cambridge University Press), 1-279
Hildebrand, A. R. 1993, J.R.A.S. Canada, 87, 77
Hildebrand, A. R., Penrield, G. T., Kring, D. A., Pilkington, M., Camargo, Z. A., Jacobsen, S. B., & Boynton, W. V. 1991, Geology, 19, 867
Hodge, P. 1994, Meteorite Craters and Impact Structures of the Earth (Cambridge, UK: Cambridge University Press)
Jansa, L. F., Aubry, M. P., & Gradstein, F. M. 1990, in Global Catastrophes in Earth History, ed. Sharpton, V. L. & Ward, P. D. (Boulder: Geological Society of America), 223
Joachimski, M. M., & Buggisch, W. 2001, Ceme. Conf., No.3072
Krinov, E. L. 1971, Meteoritics, 6, 127
Master, S., & Reimold, W. U. 2001, Ceme. Conf., No.3099
McDonald, I., Andreoli, M. A. G., Hart, R. J., & Tredoux, M. 2000, Ceme. Conf., No.3100
McEwen, A. S., Moore, J. M., & Shoemaker, E. M. 1997, JGR, 102, 255
Moilanen, J. 2001, List of Impact Structures of the World, http://www.netppl.fi/ jarmom/geo/imp/impactlist.htm
Montanari, A., Bagatin, A. C., & Farinella, P. 1998, Planet. Space Sci., 46, 271
Morrow, J. R., & Sandberg, C. A. 2001, LPI Conf. Ser., 32, 1223
Neukum, G., Ivanov, B. A., & Hartmann, W. K. 2001, Space Sci. Rev., 96, 55
Schnetzler, C., & Honey, F. 1998, LPI Conf. Ser., 19, 375
Sharpton, V. L., Burke, K., Camargo-Zanoguera, A., Hall, S. A., Lee, D. S., Marin, L. E., Suarez-Reynoso, G., Quezada-Muneton, J. M., Spudis, P. D., & Urrutia-Fucugauchi, J. 1993, Science, 261, 1564
Shoemaker, E. M. 1998, J.R.A.S. Canada, 92, 297
Strom, R. G. 1998, LPI Conf. Ser., 19, 1141
USGS 2001, Principal Lunar Craters, http://www.fourmilab.ch/earthview/lunarform/cratallp.html

# APPENDIX

Table 1. Terrestrial Impact Crater List (2001)

| No. | CRATER NAME | LOCATION | LATITUDE | LONGITUDE | AGE (Myr) | ERROR (Myr) | DIAMETER (km) |
|---|---|---|---|---|---|---|---|
| 1 | SUAVJARVI | Russia | N 63 07 | E 33 23 | 2400 | – | 16 |
| 2 | VREDEFORT | South Africa | S 27 00 | E 27 30 | 2023(2018?) | ±4 | 250–300(140?) |
| 3 | KGAGODI | Botswana | S 22 29 | E 27 35 | <2000 | – | 3.5 |
| 4 | PAASSELKA | Finland | N 62 12 | E 29 23 | <1900 | – | 10 |
| 5 | SUDBURY | Canada | N 46 36 | W 81 11 | 1850 | ±3.00 | 200 (250?) |
| 6 | SHOEMAKER (or Teague) | Australia | S 25 52 | E 120 53 | 1685 | ±5 | 30 |
| 7 | LYCKSELE | Sweden | N 64 55 | E 18 47 | 1800–1260 | – | 130 |
| 8 | BJORKO | Sweden | N 59 24 | E 17 35 | 1210 | – | 9 |
| 9 | LANDSORTSJUPET | Sweden | N 58 47 | E 18 30 | 1200 | – | 30 |
| 10 | HIGHBURY | Zimbabwe | S 17 05 | E 30 09 | 1034 | ±13(17?) | 20(25?) |
| 11 | ISO-NAAKKIMA | Finland | N 62 11 | E 27 09 | 1000 | – | 3 |
| 12 | ZHAMANSHIN | Kazakhstan | N 48 24 | E 60 58 | 900 | ±100 | 13.5 |
| 13 | LUMPARN | Finland | N 60 08 | E 20 07 | 500–1200 | – | 9 (7–10?) |
| 14 | JANISJARVI | Russia | N 61 58 | E 30 55 | 698 | ±22.00 | 14 |
| 15 | STRANGWAYS | Australia | S 15 12 | E 133 35 | 646 | ±42 | 25 |
| 16 | SAARIJARVI | Finland | N 65 17 | E 28 25 | >600 | | 1.4 (2?) |
| 17 | BEAVERHEAD | Montana, USA | N 44 36 | W 113 00 | 600 | – | 60 |
| 18 | MISARAI | Lithuania | N 54 00 | E 23 54 | 595 (395±145?) | ±50.00 | 5 |
| 19 | ACRAMAN | Australia | S 32 01 | E 135 27 | >570 | – | 90 (160?) |
| 20 | SPIDER | Australia | S 16 44 | E 126 05 | 570 (>720) | – | 13 |
| 21 | AVIKEBUKTEN | Sweden | N 62 30 | E 17 41 | <570 | – | 9.5 |
| 22 | TRINDJUPET | Sweden | N 64 12 | E 22 24 | <570 | – | 5 |
| 23 | SODERFJARDEN | Finland | N 63 00 | E 21 35 | 560 (550?) | – | 5.5 (5–6?) |
| 24 | HOLLEFORD | Canada | N 44 28 | W 76 38 | 550 | ±100.00 | 2.35 |
| 25 | KELLY WEST | Australia | S 19 56 | E 133 57 | 550 | – | 10 |
| 26 | SAAKSJARVI | Finland | N 61 24 | E 22 24 | 543 (510–514?) | ±12.00 | 5 |
| 27 | HUMMELN | Sweden | N 57 24 | E 16 18 | 520 | – | 2 |
| 28 | LAWN HILL | Australia | S 18 40 | E 138 39 | 515 | – | 18 |
| 29 | GARDNOS | Norway | N 60 39 | E 09 12 | 500 | ±10 | 5 |
| 30 | GLOVER BLUFF | USA | N 43 58 | W 89 32 | <500 | – | 10 (3?) |
| 31 | PRESQU'ILE | Canada | N 49 43 | W 78 48 | <500 | – | 12 |
| 32 | NEWPORTE | N. Dakota, U | N 48 58 | W 101 58 | <500 | – | 3.2 |
| 33 | VERSAILLES | Kentucky, US | N 38 02 | W 84 42 | <400 | – | 1.5 |
| 34 | NEUGRUND | Estonia | N 59 20 | E 23 31 | 474 | – | 5 (6–8?) |
| 35 | AMES | Oklahoma USA | N 36 15 | W 98 10 | 470 | ±30 | 16 |
| 36 | GRANDBY | Sweden | N 58 25 | E 15 56 | 470 | ±30.00 | 3 |
| 37 | CALVIN | USA | N 41 50 | W 85 57 | 460 | ±10.00 | 8.5 (7?) |
| 38 | KARDLA | Estonia | N 58 59 | E 22 40 | 455 | – | 4 |
| 39 | LOCKNE | Sweden | N 63 00 | E 14 48 | 455 | – | 13.5 |
| 40 | TVAREN BAY | Sweden | N 58 46 | E 17 25 | 455 | – | 2 |
| 41 | BRENT | Canada | N 46 05 | W 78 29 | 450 | ±30.00 | 3.8 |
| 42 | LUKANGA | Zambia | S 14 24 | E 27 45 | 500–300 | – | 110 |
| 43 | PILOT LAKE | Canada | N 60 17 | W 111 01 | 445 | ±2.00 | 6 (5.8?) |
| 44 | SLATE ISLANDS | Canada | N 48 40 | W 87 00 | 436 | – | 32 |
| 45 | COUTURE | Canada | N 60 08 | W 75 20 | 430 | 25 | 8 |
| 46 | LAC COUTURE | Canada | N 60 08 | W 75 20 | 430 | ±25.00 | 8 |
| 47 | GLASFORD | USA | N 40 36 | W 89 47 | <430 | | 4 |
| 48 | LAC LA MOINERIE | Canada | N 57 26 | W 66 37 | 400 | ±50.00 | 8 |
| 49 | NICHOLSON LAKE | Canada | N 62 40 | W 102 41 | <400 | – | 12.5 |
| 50 | ILYINETS | Ukraine | N 49 06 | E 29 12 | 395 | ±5 | 4.5 |
| 51 | KALUGA | Russia | N 54 30 | E 36 15 | 380 | ±10.00 | 15 |
| 52 | SILJAN | Sweden | N 61 02 | E 14 52 | 368 | ±1.10 | 55 (52?) |
| 53 | ALAMO | USA | N 37 30 | W 116 30 | 367 | – | 190 |
| 54 | FLYNN CREEK | USA | N 36 17 | W 85 40 | 360 | ±20.00 | 3.55 |
| 55 | MISHINA GORA (or Mishinogorsk) | Russia | N 58 40 | E 28 00 | 360 | – | 4.5 (4?) |

Table 1. Continued.

| No. | CRATER NAME | LOCATION | LATITUDE | LONGITUDE | AGE (Myr) | ERROR (Myr) | DIAMETER (km) |
|---|---|---|---|---|---|---|---|
| 56 | PICCANINNY | Australia | S 17 32 | E 128 25 | <360 | – | 7 |
| 57 | CHARLEVOIX | Canada | N 47 32 | W 70 18 | 357 | ±15 | 54 |
| 58 | GWENI-FADA | Chad | N 17 25 | E 21 45 | <345 | – | 14 |
| 59 | CROOKED CREEK | USA | N 37 50 | W 91 23 | 320 | ±80.00 | 7 |
| 60 | SERPENT MOUND | USA | N 39 02 | W 83 24 | 320 | – | 8 (6.4?) |
| 61 | KENTLAND | Indiana, USA | N 40 45 | W 87 24 | 300 | – | 13 |
| 62 | SERRA DA CANGALHA | Brazil | S 08 05 | W 46 52 | <300 | – | 12 |
| 63 | DECATURVILLE | USA | N 37 54 | W 92 43 | <300 | – | 6 |
| 64 | ILE ROULEAU | Canada | N 50 41 | W 73 53 | <300 | – | 4 |
| 65 | MIDDLESBORO | USA | N 36 37 | W 83 44 | <300 | – | 6 |
| 66 | CLEARWATER LAKE EAST | Canada | N 56 05 | W 74 07 | 290 | ±20 | 22 |
| 67 | CLEARWATER LAKE WEST | Canada | N 56 13 | W 74 30 | 290 | ±20 | 32 |
| 68 | TERNOVSKAYA | Ukraine | N 48 01 | E 33 05 | 280 | ±10.00 | 12 |
| 69 | DES PLAINES | USA | N 42 03 | W 87 52 | <280 | – | 8 |
| 70 | WOODLEIGH | Australia | S 26 05 | E 114 43 | 280–250 (305?) | (±55.00?) | 120 |
| 71 | KURSK | Russia | N 51 40 | E 36 00 | 250 | ±80.00 | 5.5 |
| 72 | GOW LAKE | Canada | N 56 27 | W 104 29 | <250 | – | 5 (4?) |
| 73 | LAKE KARIKKOSELKA | Finland | N 62 13 | E 25 15 | 260-230 | – | 2.4 |
| 74 | ARAGUAINHA DOME | Brazil | S 16 46 | W 52 59 | 243(249?) | ±19 | 40 |
| 75 | KARIKKOSELKA | Finland | N 62 13 | E 25 14 | 230 | – | 1.4 (1.2–1.5?) |
| 76 | PUCHEZH-KATUNSKII | Russia | N 57 06 | E 43 35 | 220 | ±10 | 80 |
| 77 | SINAMWENDA | Zimbabwe | S 17 12 | E 27 47 | <220 | – | 0.22 |
| 78 | SAINT MARTIN | Canada | N 51 47 | W 98 32 | 219.5 | ±32.00 | 40 |
| 79 | OBOLON | Ukraine | N 49 30 | E 32 55 | 215 | ±25 | 15 |
| 80 | ROCHECHOUART | France | N 45 50 | E 00 56 | 214 | ±8 | 23 |
| 81 | MANICOUAGAN | Canada | N 51 23 | W 68 42 | 214 (212?) | ±1.00 | 100 |
| 82 | DOBELE | Latvia | N 56 35 | E 23 15 | 205 (300?) | ±35.00 | 4.5 |
| 83 | RED WING | N. Dakota, U | N 47 36 | W 103 33 | 200 | ±25 | 9 |
| 84 | RIACHAO RING | Brazil | S 07 43 | W 46 39 | 200 | – | 4.5 |
| 85 | VIEWFIELD | Canada | N 49 35 | W 103 04 | 200 | – | 2.4 |
| 86 | WELLS CREEK | USA | N 36 23 | W 87 40 | 200 | ±100.00 | 12 (14?) |
| 87 | VEPRIAJ | Lithuania | N 55 06 | E 24 36 | 165 | ±30.00 | 7.5 (8?) |
| 88 | LIVERPOOL | Australia | S 12 24 | E 134 03 | 150 | ±70.00 | 1.6 |
| 89 | MOROKWENG | South Africa | S 26 28 | E 23 32 | 145 | ±0.8 | 70-80 |
| 90 | MJILNIR | Barents Sea | N 73 48 | E 29 40 | 143 | ±20 | 40 |
| 91 | GOSSES BLUFF | Australia | S 23 50 | E 132 19 | 142.5 | ±0.50 | 22 |
| 92 | ROTMISTROVKOGO | Ukraine | N 49 00 | E 32 00 | 140 | ±20.00 | 2.7 |
| 93 | GOYDER | Australia | S 13 29 | E 135 02 | >136.0 | – | 3 |
| 94 | AZUARA | Spain | N 41 10 | W 00 55 | <130 | – | 30 (40?) |
| 95 | DUOLUN | China | N 42 03 | E 116 15 | 129 | ±3 | 70 |
| 96 | TOOKOONOOKA | Australia | S 27 00 | E 143 00 | 128 | ±5 | 55 |
| 97 | MIEN | Sweden | N 56 25 | E 14 52 | 121 | ±2.30 | 9 |
| 98 | ZELENY GAI | Ukraine | N 48 42 | E 32 54 | 120 (>140?) | ±20.00 | 2.5 |
| 99 | BP STRUCTURE | Libya | N 25 19 | E 24 20 | <120 | – | 2.8 |
| 100 | OASIS | Libya | N 24 35 | E 24 24 | <120 | – | 11.5 |
| 101 | CARSWELL | Canada | N 58 27 | W 109 30 | 115 | ±10.00 | 39 |
| 102 | ZAPADNAYA | Ukraine | N 49 44 | E 29 00 | 115 | ±10 | 4 |
| 103 | AVAK | Alaska, USA | N 71 15 | W 156 38 | 100 | ±5 | 12 |
| 104 | WEST HAWK LAKE | Canada | N 49 46 | W 95 11 | 100 | ±50.00 | 2.44 (3.15?) |
| 105 | DEEP BAY | Canada | N 56 24 | W 102 59 | 100 (150) | ±50.00 | 13 (10?) |
| 106 | MOUNT TOONDINA | Australia | S 27 57 | E 135 22 | <110 | – | 4 (3?) |
| 107 | SIERRA MADERA | USA | N 30 36 | W 102 55 | <100 | – | 13 |
| 108 | STEEN RIVER | Canada | N 59 31 | W 117 37 | 95 | ±7.00 | 25 |
| 109 | DELLEN | Sweden | N 61 55 | E 16 39 | 89 (110?) | ±2.70 | 19 (15?) |
| 110 | BOLTYSH | Ukraine | N 48 45 | E 32 10 | 88 | ±3.00 | 24 (25?) |

Table 1. Continued.

| No. | CRATER NAME | LOCATION | LATITUDE | LONGITUDE | AGE (Myr) | ERROR (Myr) | DIAMETER (km) |
|---|---|---|---|---|---|---|---|
| 111 | WETUMPKA | USA | N 32 31 | W 86 11 | 81.5 | ±1.5 | 6.5 |
| 112 | LAPPAJARVI | Finland | N 63 09 | E 23 42 | 77.3 | ±0.40 | 17 (23?) |
| 113 | MANSON | USA | N 42 35 | W 94 31 | 74 (65.70±1?) | – | 35 |
| 114 | KARA | Russia | N 69 05 | E 64 18 | 70.3 | ±2.20 | 65 |
| 115 | UST-KARA | Russia | N 69 18 | E 65 18 | 70.3 | ±2.2 | 25 |
| 116 | VARGEAO DOME | Brazil | S 26 50 | W 52 07 | <70 | – | 12 |
| 117 | CHUKCHA | Russia | N 75 42 | E 97 48 | <70 | – | 6 |
| 118 | OUARKZIZ | Algeria | N 29 00 | W 07 33 | <70 | – | 3.5 |
| 119 | TIN BIDER | Algeria | N 27 36 | E 05 07 | <70 | – | 6 |
| 120 | BEYENCHIME-SALAATIN | Russia | N 71 50 | E 123 30 | 65 | – | 8 (7.5?) |
| 121 | GUSEV | Russia | N 48 21 | E 40 14 | 65 | – | 3.5 |
| 122 | KAMENSK | Russia | N 48 20 | E 40 15 | 65 | ±2.00 | 25 |
| 123 | UPHEAVAL DOME | Utah, USA | N 38 26 | W 109 54 | 65 | – | 5 |
| 124 | EAGLE BUTTE | Canada | N 49 42 | W 110 35 | <65 | – | 19 |
| 125 | CHICXULUB | Mexico | N 21 20 | W 89 30 | 64.98 | ±0.05 | 170 |
| 126 | CONNOLLY BASIN | Australia | S 23 32 | E 124 45 | <60 | – | 9 |
| 127 | HICO | Texas, USA | N 32 00 | W 98 02 | <60 | | 9 |
| 128 | MARQUEZ DOME | USA | N 31 17 | W 96 18 | 58 | ±2.00 | 13 (13–22?) |
| 129 | RAGOZINKA | Russia | N 58 18 | E 62 00 | 55 | ±5.00 | 9 |
| 130 | MONTAGNAIS | W. Atlantic | N 42 53 | W 64 13 | 50.5 | ±0.76 | 45 |
| 131 | GOAT PADDOCK | Australia | S 18 20 | E 126 40 | 50 (55?) | – | 5.1 |
| 132 | CHIYLI | Kazakstan | N 49 10 | E 57 51 | 46 | ±7.00 | 5.5 (3?) |
| 133 | LOGOISK | Belorussia | N 54 12 | E 27 48 | 40 | ±5.00 | 17 |
| 134 | BEE BLUFF | USA | N 29 2 | W 99 51 | <40 | – | 2.4 |
| 135 | MISTASTIN Lake | Canada | N 55 53 | W 63 18 | 38 | ±4.00 | 28 |
| 136 | WANAPITEI LAKE | Canada | N 46 45 | W 80 45 | 37 | ±2 | 7.5 |
| 137 | POPIGAI | Russia | N 71 30 | E 110 00 | 35.7 | ±0.2 | 100 |
| 138 | CHESAPEAKE BAY | Virginia, US | N 37 15 | W 76 05 | 35.5 | ±0.6 | 85 |
| 139 | TOM'S CANYON | W. Atlantic | N 39 08 | W 72 51 | 35.5 | ±0.3 | 15-20 |
| 140 | FOHN | Timor Sea | S 13 15 | E 128 39 | 36.0-24.6 | – | 4.8 |
| 141 | LOGANCHA | Russia | N 65 30 | E 95 48 | 25 | ±20.00 | 20 (50?) |
| 142 | KARA-KUL | Tajikistan | N 39 01 | E 73 27 | 25 (<10?) | – | 52 (45?) |
| 143 | HAUGHTON | Canada | N 75 22 | W 89 41 | 23.4 (21.4?) | ±1.00 | 24 (20.5?) |
| 144 | TAKAMATSU | Japan | N 34 26 | E 134 05 | 15.3 | – | 4 |
| 145 | RIES | Germany | N 48 53 | E 10 37 | 14.87 (14.1?) | ±0.36 | 24 |
| 146 | STEINHEIM | Germany | N 48 40 | E 10 04 | 14.8 | ±0.70 | 3.8 (3.4?) |
| 147 | SHUNAK | Kazakstan | N 47 12 | E 72 42 | 12 | ±5.00 | 3.1 |
| 148 | KARLA | Russia | N 54 54 | E 48 00 | 10 | – | 12 |
| 149 | BIGACH | Kazakstan | N 48 30 | E 82 00 | 6 | ±3.00 | 7 |
| 150 | ROTER KAMM | Namibia | S 27 46 | E 16 18 | 3.7 | ±0.30 | 2.5 (5?) |
| 151 | EL'GYGYTGYN | Russia | N 67 30 | E 172 05 | 3.58 | ±0.04 | 18 |
| 152 | AOUELLOUL | Mauritania | N 20 15 | W 12 41 | 3.1 | ±0.30 | 0.36(0.39) |
| 153 | TABUN-KHARA-OBO | Mongolia | N 44 06 | E 109 36 | 3 (>120?) | – | 1.3 |
| 154 | TALEMZANE | Algeria | N 33 19 | E 04 02 | <3.0 | – | 1.75 |
| 155 | TENOUMER | Mauritania | N 22 55 | W 10 24 | 2.5 | ±0.50 | 1.9 |
| 156 | ELTANIN | Pacific | S 57 47 | W 90 47 | 2.15 | – | 15–20 (?) |
| 157 | KALKKOP | South Africa | S 32 43 | E 24 34 | <1.8 | – | 0.64 |
| 158 | *NEW QUEBEC (or Nunavik)* | *Canada* | N 61 17 | W 73 40 | 1.4 | ±0.1 | 3.44 |
| 159 | PINGUALUIT | Canada | N 61 17 | W 73 40 | 1.4 | ±0.10 | 3.44 |
| 160 | BOSUMTWI | Ghana | N 06 32 | W 01 25 | 1.1 | ±0.2 | 10.5 (12?) |
| 161 | MONTURAQUI | Chile | S 23 56 | W 68 17 | 1.0 | – | 0.46 |
| 162 | VEEVERS | Australia | S 22 58 | E 125 22 | <1.0 | – | 0.08 |
| 163 | SIMUNA | Estonia | N 58 54 | E 25 36 | 0.82(Quat.) | ±0.22 | 0.0089 |
| 164 | TANNAS | Sweden | N 62 24 | E 12 42 | 0.82(Quat.) | ±0.22 | 20 |
| 165 | DARWIN CRATER | Tasmania | S 42 18 | E 145 40 | 0.81 | ±0.04 | 1 |

Table 1. Continued.

| No. | CRATER NAME | LOCATION | LATITUDE | LONGITUDE | AGE (Myr) | ERROR (Myr) | DIAMETER (km) |
|---|---|---|---|---|---|---|---|
| 166 | DARWIN | Australia | S 42 18 | E 145 40 | 0.73 | – | 1 |
| 167 | WOLFE CREEK | Australia | S 19 18 | E 127 46 | <0.30 | – | 0.875 |
| 168 | PRETORIA SALTPAN (or Tswai) | S Africa | S 25 24 | E 28 05 | 0.20 | – | 1.13 |
| 169 | RIO CUARTO | Argentina | S 30 52 | W 64 14 | 0.10 | – | 4.5 |
| 170 | AMGUID | Algeria | N 26 05 | E 04 23 | <0.10 | – | 0.45 |
| 171 | ODESSA | USA | N 31 45 | W 102 29 | <0.05 | – | 0.168 |
| 172 | AMBAR LAKE | India | N 19 59 | E 76 31 | 0.052 | ±0.006 | 0.3 |
| 173 | LONAR | India | N 19 59 | E 76 31 | 0.052 | ±0.006 | 1.83 |
| 174 | BARRINGER | Arizona, USA | N 35 02 | W 111 01 | 0.049 | – | 1.186 |
| 175 | DALGARANGA | Australia | S 27 45 | E 117 05 | 0.03 | – | 0.021 |
| 176 | BOXHOLE | Australia | S 22 37 | E 135 12 | 0.03 (0.005) | – | 0.185 |
| 177 | MACHA | Russia | N 59 59 | E 118 00 | 0.01 | – | 300 |
| 178 | MORASKA | Poland | N 52 29 | E 16 54 | 0.01 | – | 0.1 |
| 179 | SYTHYLEMENKAT LAKE | Alaska, USA | N 66 07 | W 151 23 | 0.01 | – | 12 |
| 180 | AOROUNGA | Chad | N 19 06 | E 19 15 | 0.01(200–360?) | – | 12.6 |
| 181 | TSOORIKMAE | Estonia | N 58 06 | E 27 30 | 0.0095 | – | 0.04 |
| 182 | KAALIJARV | Estonia | N 58 24 | E 22 40 | 0.0075 | – | 0.11 |
| 183 | ILUMETSA | Estonia | N 57 58 | E 25 25 | >0.006 | – | 0.08 |
| 184 | HENBURY | Australia | S 24 35 | E 133 09 | <0.005 (0.001?) | – | 0.157 |
| 185 | CAMPO DEL CIELO | Argentina | S 27 38 | W 61 42 | <0.004 | – | 50 |
| 186 | TOR | Sweden | N 62 31 | E 12 38 | 0.002 | ±0.0004 | 0.02 |
| 187 | HAVILAND | USA | N 37 35 | W 99 10 | <0.001 | – | 0.015 |
| 188 | SOBOLEV | Russia | N 46 18 | E 138 52 | 0.0002 | – | 0.053 |
| 189 | WABAR | Saudi Arabia | N 21 30 | E 50 28 | 0.0064 | ±0.0026 | 0.116, 0.064, 0.01 |
| 190 | SIKHOTE-ALIN | Russia | N 46 07 | E 134 40 | 12-Feb-47 | – | 0.027 |
| 191 | STERLITAMAK | Russia | N 53 40 | E 55 59 | 17-May-90 | – | 0.0094 |
| 192 | KUNYA-URGENCH | Turkmenistan | N 42 15 | E 59 12 | 20-Jun-98 | – | 0.006 |